Accepted Manuscript

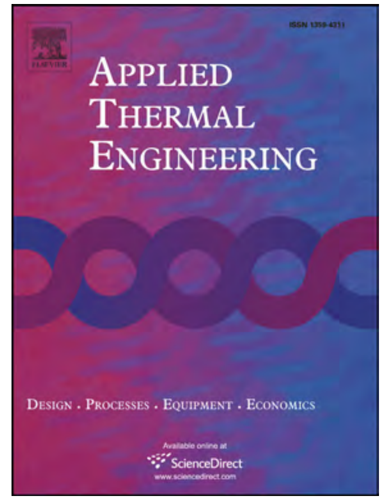

Controlled variable analysis of counter flow heat exchangers based on thermodynamic derivation

Yunli Jin, Naiping Gao, Tong Zhu

PII: S1359-4311(17)33993-5
DOI: https://doi.org/10.1016/j.applthermaleng.2017.10.025
Reference: ATE 11223

To appear in: *Applied Thermal Engineering*

Received Date: 13 June 2017
Revised Date: 25 September 2017
Accepted Date: 4 October 2017

Please cite this article as: Y. Jin, N. Gao, T. Zhu, Controlled variable analysis of counter flow heat exchangers based on thermodynamic derivation, *Applied Thermal Engineering* (2017), doi: https://doi.org/10.1016/j.applthermaleng.2017.10.025

Controlled variable analysis of counter flow heat exchangers based on thermodynamic derivation

Yunli Jin, Naiping Gao*, Tong Zhu

School of Mechanical Engineering, Tongji University, Shanghai 201804, China

*Corresponding author: Naiping Gao;

Tel: 86-21-65983867;

Email address: gaonaiping@tongji.edu.cn;

Postal address: School of Mechanical Engineering, Tongji University, No. 4800 Cao'an Road, Shanghai 201804, China

Abstract

To optimize the controlled variable of counter flow heat exchanger, T-Q diagram inducing entropy angle and thermal capacity angle is used to analyze heat exchange process. The results show that selecting stream outlet temperature as controlled variable is incapable of perceiving overall variation of thermal capacity flow rates. The change of heat exchanger effectiveness isn't completely consistent with heat transfer irreversibility, and cannot reflect the effect of remanent (flow-imbalance) irreversibility. The terminal temperature difference imposed by heat transfer irreversibility $N_{s,\Delta T}$ is the same at both ends. However, the remanent irreversibility $N_{s,imb}$ makes the terminal temperature difference of one end deviate from the other. Based on maximizing the heat exchange amount and minimizing the irreversible loss, a new controlled variable τ named as heat exchanger comprehensive effectiveness is constructed, which is easy to be measured and calculated. It can reflect the effect of heat exchanger effectiveness, remanent

irreversibility, and heat transfer irreversibility simultaneously.

Keywords:

Counter flow heat exchanger; Controlled variable; Heat exchanger effectiveness; Remanent irreversibility; Heat transfer irreversibility

Nomenclature			
A	surface area, m^2	*Greeks*	
c	specific heat, J/kg K	β	entropy angle
c_p	specific heat at constant pressure, J/kg K	ε	effectiveness
K	overall heat transfer coefficient, $\mathrm{W/m^2K}$	θ	terminal temperature difference
$\dot{m}$	mass flow rate, kg/s	τ	comprehensive effectiveness
N_s	entropy generation number	φ	thermal capacity angle
NTU	number of heat transfer units		
P	pressure, Pa	*Subscripts*	
Q	heat transfer, J	c	cold stream
$\dot{Q}$	heat transfer rate, W	h	hot stream
R	thermal capacity flow rate ratio	imb	imbalance thermal capacity flow rate
s	specific entropy, J/kg K	in	inlet
S	entropy, J/K	max	maximum
$\dot{S}_{gen}$	entropy generation rate, W/K	out	outlet
T	temperature, K	ΔP	pressure drop
ΔT_m	average heat transfer temperature difference, K	s	entropy

1. Introduction

Heat exchanger is the key component of heating and cooling system which is widely used in industrial field. Counter flow heat exchanger is the study object of this paper. Heat exchangers normally work under various conditions, so the control system should adjust accordingly the controlled variable by changing manipulated variable.

The control strategies of counter flow heat exchanger have been studied in recent years. The functional predictive control was applied to a counter flow heat exchanger by Arbaoui et al. [1]. The cold stream outlet temperature was adopted as the controlled variable and the hot stream flow rate as the manipulated variable. The functional predictive control used an approximated first order nonlinear dynamic model. The gain and time constant of the model change with hot stream flow rate. Abu-Hamdeh [2] proposed a dual-input and dual-output control of liquid-liquid counter flow heat exchanger. The outlet temperatures of cold and hot stream were controlled respectively by manipulating the corresponding flow rate. The influence of one side on the other was decoupled by a non-interactive controller. A feed-forward controller was introduced to overcome the inlet temperature disturbances. Heo et al. [3] presented an input/output linearizing controller for high-duty counter flow heat exchangers based on both the original stiff model and the reduced non-stiff model. The outlet temperature of hot stream was controlled by manipulating the flow rate of cold stream. Maidi et al. [4] investigated the boundary geometric control of a counter flow heat exchanger. The results showed that the outlet temperature of the internal fluid could be very well controlled by manipulating the inlet temperature of external fluid, which provided better performance than by manipulating mass flow rate.

Control optimization of counter flow heat exchanger was carried out by Burns et al [5-8]. In their research, the heat exchanger model including actuator dynamics was built to evaluate the impact of introducing full-flux terms on controller design. The model was governed by a parabolic partial differential equation with boundary input originating from an actuator output governed by a delay differential equation [5-6]. To low flow, a composite finite element - finite volume scheme to produce finite dimensional systems was used [7]. They also developed a numerical scheme based on average approximations applied to optimal control [8].

For these control strategies which use inlet temperature and mass flow rate as manipulated variables and feed-forward variables, it is very important to obtain the system dynamic responses to the change of them. Ansari [9] applied a numerical method based on the analytical solution of energy equation to analyze the system responses. For control algorithm design, Feru et al. [10] developed a counter flow heat exchanger model based on finite volume formulation to capture the dynamic phenomena of two-phase fluid flow. Lakshmanan et al. [11] developed the Cinematic model utilizing analytical solutions to simulate the dynamic behavior of a counter flow heat exchanger. It is also essential to obtain the effect of inlet temperature and mass flow rate on system performance and outlet parameters. The influence of mass flow rate on temperature distributions along a tubular counter flow heat exchanger was studied by Abdelghani-Idrissi et al. [12]. The effect of inlet temperature and mass flow rate variation of both sides on the outlet temperatures was investigated by Laskowski [13]. The experiments and model analysis conducted by Naphon [14] showed that the inlet temperatures and mass flow rates of both sides had significant effect on heat transfer characteristics, entropy generation, and exergy loss.

As mentioned above, the previous studies of heat exchanger control almost all focused on the control algorithm, but rarely involved the controlled variables optimization. The outlet temperatures of hot steam and cold stream are normally used as the controlled variable of coolers and heaters respectively. The inlet temperature is only used as feed-forward signal to reduce the response delay of outlet temperature. However, only selecting outlet temperature as controlled variable has limitations which couldn't fully reflect the heat exchanger effectiveness and irreversibility. For example, hot stream varies in view of inlet temperature and thermal capacity flow rate, and cold stream outlet temperature is selected as controlled variable. If for the purpose is to maximize the heat exchange and minimize the irreversible loss, the set-point of cold stream outlet temperature has to closely follow hot stream inlet temperature which complicates the control. When the thermal capacity flow rate of the hot stream is already larger than the cold stream and continues to increase under the situation of *NTU* approaching infinity, the cold stream outlet temperature variation could be very small. In effect, the outlet temperature of one side is not sensitive to the thermal capacity flow rate of the other side if the thermal capacity flow rate is already higher than the current side when *NTU* is very large.

The controlled variables should be able to evaluate the performance of heat exchanger in real time. The evaluation criterions of performance usually include effectiveness, entropy generation (irreversibility) and exergy [15]. Lerou et al. [16] treated all losses of counter flow heat exchanger as an entropy production. Then an optimal configuration of counter flow heat exchanger was obtained by minimizing the entropy production. Ordonez et al. [17] optimized a counter flow heater by minimizing the entropy generation through adjusting the two-channel spacing ratio, the total heat transfer area, and the thermal capacity rates ratio. The optimization was robust to whether including external discharge irreversibility into entropy generation rate or not. The change trends of entropy generation and effectiveness aren't always consistent.

Mohamed [18] derived that the irreversibility peak value appeared at half of the maximum effectiveness for balanced heat exchangers, but it depended on thermal capacity flow rate ratio for imbalanced heat exchangers. Xu [19] investigated the difference between the available energy loss and the irreversibility of counter flow heat exchangers. The results showed the change trends of them were obviously different. The change of exergy isn't consistent with effectiveness and entropy. San [20] proposed exergy recovery index (η_{II}) defined as the net recovered thermal exergy divided by the available thermal exergy in the hot stream, to evaluate the second law performance of heat exchangers. The exergy recovery index was expressed as a function of effectiveness, heat capacity rate ratio, hot and cold stream inlet temperatures and overall pressure drop factor. The results showed that under the same effectiveness, exergy recovery index still changed with the capacity rate ratio of hot stream to cold stream. Gupta et al. [21] observed that the internal exergy loss decreased if heat transfer unit number increased and the cold fluid was the fluid with minimum capacity rate, but became nearly constant with heat transfer unit number increasing if the hot fluid was the fluid with minimum capacity rate. The results are different from the change trends of entropy generation number and effectiveness with heat transfer unit number described by Bejan [22].

As discussed above, none of effectiveness, entropy generation, and exergy can represent independently the comprehensive performance of a counter flow heat exchanger. Moreover, they are all involved in mass flow rate which sometimes is difficult to be measured accurately and their calculations are too complicated to be controlled variables.

This paper puts emphasis on the controlled variable optimization of counter flow heat exchangers already designed and integrated into systems. In many circumstances studied in this paper, the operation demand of a heat exchanger is to recover heat from a hot stream as much as possible and degrade thermal energy quality as little as possible. In these cases, the objective of constructing controlled variables is to maximize the heat exchange amount and minimize the irreversible loss. The requirements to the controlled variables include two parts. One is easy to be measured accurately and calculated. The other is that it can cover all the influences of effectiveness and irreversibility.

A new controlled variable τ is constructed in this paper based on *T-Q* diagram analysis. The *T-Q* diagram introduces entropy angle and thermal capacity angle, which makes it much clearer and easier to discuss the influence of related parameters on heat transfer process. The controlled variable τ can reflect the heat exchanger effectiveness, remanent irreversibility, and heat transfer irreversibility simultaneously. The computation of this new controlled variable just requires the stream inlet and outlet temperatures of both sides, thus simplifying the online measurement.

2. Mathematical formulation

The counter flow surface heat exchanger, as shown in Fig.1, is studied in this paper. It is assumed that the phase transformation doesn't occur and the thermal capacity flow rates keep constant along the heat transfer surface. The fluid flow irreversibility $(N_{s,\Delta P})$ is assumed to be negligible comparing with remanent irreversibility $(N_{s,imb})$ and heat transfer irreversibility $(N_{s,\Delta T})$.

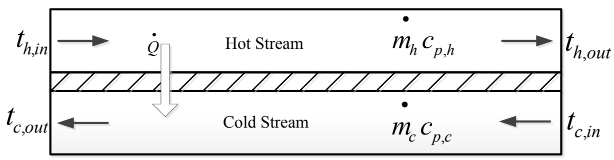

Fig.1 Schematic drawing of the counter flow surface heat exchanger

The heat exchanger effectiveness is defined as:

$$\varepsilon = \frac{(\dot{m}c_p)_c(T_{c,out}-T_{c,in})}{(\dot{m}c_p)_{min}(T_{h,in}-T_{c,in})} = \frac{(\dot{m}c_p)_h(T_{h,in}-T_{h,out})}{(\dot{m}c_p)_{min}(T_{h,in}-T_{c,in})} \quad (1)$$

where $\dot{m}c_p$ represents the thermal capacity flow rate, $T_{c,in}$ and $T_{c,out}$ represent inlet and outlet temperature of the cold stream, respectively, and $T_{h,in}$ and $T_{h,out}$ represent inlet and outlet temperature of the hot stream, respectively. The work done by Laskowski [13] and Bahadori [23] all showed that the heat transfer effectiveness of counter flow heat exchanger could be expressed as a function of the heat capacity rate ratio of both fluids and the number of heat transfer units. The number of heat transfer units is given as:

$$NTU = \frac{KA}{(\dot{m}c_p)_{min}} \quad (2)$$

where *K* represents the overall heat transfer coefficient and *A* is the surface area.

If ε is selected as controlled variable to maximize the total heat exchange amount and minimize the irreversible loss, it has some limitations. Assuming the thermal resistance is zero, then at least on one end the terminal temperature difference between cold and hot streams is zero. When the thermal capacity flow rate of the cold stream is far less than the hot, the maximum available heat from the hot stream is not fully taken away by the cold stream. When the thermal capacity flow rate of the cold stream is far larger than the hot, the flow rate of cold stream exceeds the actual demand corresponding to the maximum possible releasing heat from the hot stream. However, in the two situations, ε both reaches 1 according to Eq. (1) due to the fact that at least one terminal temperature difference is zero.

The degree of thermodynamic imperfection of infinitesimal heat transfer surface is measured by the entropy generation rate:

$$d\dot{S}_{gen} = \frac{d\dot{Q}_c}{T_c} + \frac{d\dot{Q}_h}{T_h} = \frac{\dot{m}_c c_{p,c} dT_c}{T_c} + \frac{\dot{m}_h c_{p,h} dT_h}{T_h} \quad (3)$$

where $\dot{S}_{gen}$ is the entropy generation rate, $\dot{Q}_c$ is the absorbing heat transfer rate of the cold stream, $\dot{Q}_h$ is the releasing heat transfer rate of the hot stream, T_c and T_h are the heat transfer temperature of the cold and hot stream respectively. The entropy generation number N_s is defined as [22] [24]:

$$N_s = \frac{\dot{S}_{gen}}{(\dot{m}c_p)_{min}} = \frac{(\dot{S}_{gen})_{imb}+(\dot{S}_{gen})_{\Delta T}+(\dot{S}_{gen})_{\Delta P}}{(\dot{m}c_p)_{min}} = N_{s,imb} + N_{s,\Delta T} + N_{s,\Delta P} \tag{4}$$

where $N_{s,imb}$ is the entropy generation number corresponding to remanent (flow-imbalance) irreversibility, $N_{s,\Delta T}$ is the entropy generation number corresponding to heat transfer irreversibility, and $N_{s,\Delta P}$ fluid flow irreversibility. Actually, the changes of $\dot{S}_{gen}$ and N_s aren't always consistent with heat exchanger effectiveness ε.

To minimize the entropy generation according to Eq. (3), two conditions should be met. Firstly, the temperature drop of hot stream $-\mathrm{d}T_h$ equals to the temperature rise of cold stream $\mathrm{d}T_c$, which requires the thermal capacity flow rates of both sides to be equal. It means the remanent irreversibility $N_{s,imb}$ in Eq. (4) will be zero. Secondly, heat transfer temperature difference approaches zero. T_c equals to T_h, which means the heat transfer irreversibility $N_{s,\Delta T}$ is zero as well.

2.1. The remanent irreversibility

It has been proved that unequal capacity flow rates of both sides in a counter flow heat exchanger will result in the remanent irreversibility [18].

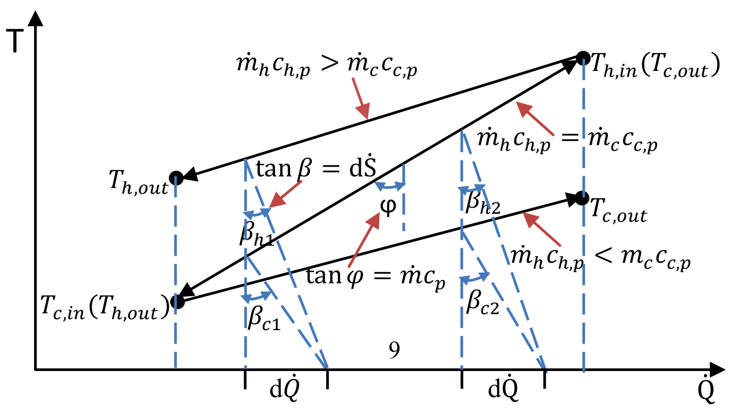

Fig.2 T-Q diagram for the counter flow heat exchanger ($NTU \to \infty$)

T-Q diagram is introduced to analyze the heat transfer process in Fig.2. In the diagram, three situations are expressed with three solid lines: the thermal capacity flow rate of hot stream is larger than, equal to or less than the cold stream. The slope of every line, $\tan\varphi$, equals to the thermal capacity flow rate. Therefore φ is defined as thermal capacity angle in this paper. Heat transfer rate $\mathrm{d}\dot{Q}$ and temperature T determine the included angle β in every infinitesimal heat exchange surface. The $\tan\beta$ equals to $\mathrm{d}\dot{S}$, thus β is named as entropy angle in this paper. For reversible process, the same heat transfer rate and temperature for hot and cold stream lead to β_c equal to β_h. Furthermore, β_c being larger than β_h means the irreversible process. T-Q diagram inducing entropy angle and thermal capacity angle can clearly reflect the difference between remanent (thermal capacity flow rate imbalance) irreversibility and heat transfer irreversibility.

NTU is assumed to approach infinity in Fig.2 which means the maximum heat transfer and minimum heat transfer temperature difference under fixed thermal capacity flow rate. Therefore, the heat transfer irreversibility $N_{s,\Delta T}$ is zero. In the first situation where $m_c c_{c,p}$ equals to $m_h c_{h,p}$, the terminal temperature differences at both ends are all zero. $T_{c,out}$=$T_{h,in}$ and $T_{h,out} = T_{c,in}$. In this case, the remanent irreversibility $N_{s,imb}$ also reaches zero. The releasing heat line of hot stream and absorbing heat line of cold stream completely overlap in Fig.2. In the second situation where $m_h c_{h,p}$ is larger than $m_c c_{c,p}$, the releasing heat line of hot stream is above the line connecting $T_{h,in}$ and $T_{c,in}$ in Fig.2. $N_{s,imb}$ increases due to the difference between entropy angle β_{c1} and β_{h1}. In the third situation in which $m_c c_{c,p}$ rises to be larger than $m_h c_{h,p}$, the absorbing heat line of cold stream is under the line connecting $T_{h,in}$ and $T_{c,in}$. The entropy angle β_{c2} and β_{h2} have a difference as well. To summarize, the thermal capacity flow rate difference at both sides inevitably leads to the entropy generation and irreversible loss that is reflected by the entropy angle difference between cold and hot stream in Fig.2.

However, for all three situations in Fig.2, ε always equals to one according to Eq. (1). As long as the stream outlet temperature at any side reaches the stream inlet temperature of the other side which means *NTU* approaches infinity, ε will always be one. This is consistent with the previous study [22]. Therefore ε couldn't reflect the irreversibility caused by thermal capacity flow rate difference. The effect of thermal capacity flow rates imbalance on heat transfer efficiency can be given as:

$$\tau_1 = \frac{N_{s,imb,max} - N_{s,imb}}{N_{s,imb,max}} \tag{5}$$

The above analysis also shows that the remanent irreversibility, caused by thermal capacity flow rate imbalance, can be reflected by the terminal temperature difference at both ends. The remanent irreversibility makes the terminal temperature difference at one end deviate from the other.

2.2. The heat transfer irreversibility

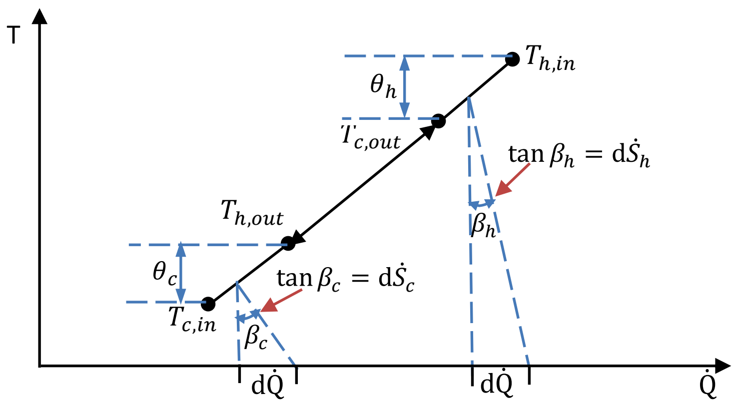

Fig.3 *T-Q* diagram for the counter flow heat exchanger ($\dot{m}_h c_{h,p} = \dot{m}_c c_{c,p}$)

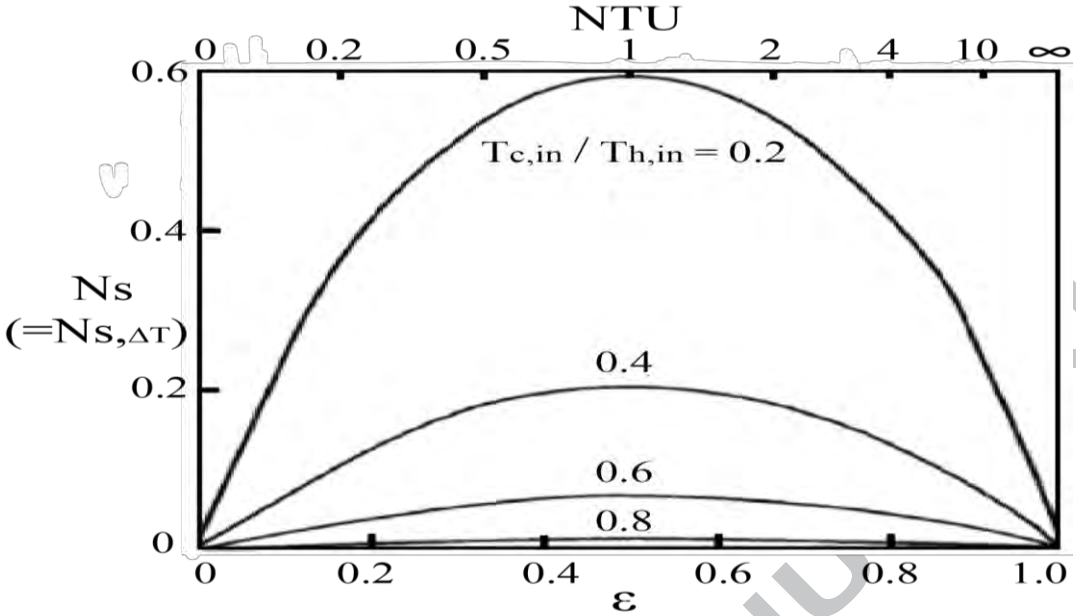

Fig.4 Entropy generation in a balanced counter flow heat exchanger with zero pressure drop irreversibility [22]

The heat transfer irreversibility $N_{s,\Delta T}$ in the case with equal thermal capacity flow rates is described in Fig.3. Fig.4 [22] is used for comparison. The remanent irreversibility $N_{s,imb}$ and pressure drop irreversibility $N_{s,\Delta P}$ are assumed to be zero in Fig.4. Thus N_s is equivalent to $N_{s,\Delta T}$. The thermal capacity flow rates of cold stream and hot stream are assumed to be equal in Fig.3 and Fig.4. Then based on Eq. (1) the following can be obtained:

$$T_{h,in} - T_{c,out} = T_{h,out} - T_{c,in} \qquad (\dot{m}_c c_{p,c} = \dot{m}_h c_{p,h}) \tag{6}$$

The cold terminal temperature difference θ_c equals to the hot terminal temperature difference θ_h in Fig.3. It can be deduced that the difference between θ_c and θ_h is originated not from heat transfer irreversibility $N_{s,\Delta T}$, but from the remanent irreversibility $N_{s,imb}$. With the equal thermal capacity flow rates, the relationship between terminal temperature difference, average heat transfer temperature difference, and *NTU* can be obtained:

$$NTU = \frac{KA(T_{h,in}-T_{c,in}-\theta)}{\dot{m}c_p(T_{h,in}-T_{c,in}-\theta)} = \frac{(T_{h,in}-T_{c,in})\varepsilon}{\Delta T_m} \qquad (\dot{m}_c c_{p,c} = \dot{m}_h c_{p,h}) \tag{7}$$

where ΔT_m is the average heat transfer temperature difference. Fixing *NTU* and ε in Eq. (7), enlarging the inlet temperature difference between hot and cold streams will lead to ΔT_m increasing. As a result, the irreversible loss increases, which explains N_s increases with $T_{c,in}/T_{h,in}$ decreasing in Fig.4.

When *NTU* reaches zero, there is no heat exchange which makes the hot and cold stream temperatures along the whole heat transfer surface equal to each inlet temperatures. Consequently, the releasing heat line of the hot stream and absorbing heat line of the cold stream both become one point in Fig.3. ε and N_s are 0 in Fig.4 due to no heat exchange.

As *NTU* increases, the rising heat exchange amount results in that the hot stream outlet temperature $T_{h,out}$ decreases towards the cold stream inlet temperature $T_{c,in}$. As shown in Fig.3, $T_{h,out}$ moves from the point $T_{h,in}$ to $T_{c,in}$ along the connecting line. $T_{c,out}$ changes as well. For equal thermal capacity flow rates, the length of absorbing heat line, connecting $T_{c,in}$ and $T_{c,out}$, is equal to the releasing heat line, connecting $T_{h,in}$ and $T_{h,out}$. The entropy angle of absorbing heat line is larger than the releasing heat line before $T_{c,out}$ meets $T_{h,out}$ in Fig.3. Therefore, $N_{s,\Delta T}$ in Fig.4 increases with the length of absorbing and releasing heat line before $T_{c,out}$ touches $T_{h,out}$. ε also increases synchronously because of the heat exchange increasing in Fig.4. Once $T_{c,out}$ meets $T_{h,out}$ as *NTU* increases, further increase of *NTU* will make releasing heat line and absorbing heat line overlap, as shown in Fig.3. Because the entropy angles of overlap section are the same, $N_{s,\Delta T}$ will stop increasing and turn to decrease with the overlap section increasing. So, at the point where $T_{c,out}$ equals to $T_{h,out}$, $N_{s,\Delta T}$ reaches the maximum in Fig.4.

When *NTU* increases to infinity, $T_{c,out}$ approaches $T_{h,in}$ and $T_{h,out}$ approaches $T_{c,in}$. The releasing heat line of the hot stream and absorbing heat line of the cold stream overlap completely in Fig.3 which means the heat transfer temperature difference covering all the heat transfer surface is zero. Under this circumstance, $N_{s,\Delta T}$ decreases to zero and ε reaches the maximum.

Because the thermal capacity flow rates of cold and hot streams are assumed to be equal, the point where $T_{c,out}$ meets $T_{h,out}$ is in the middle of the line connecting $T_{h,in}$ and $T_{c,in}$ in Fig.3. At this point, $N_{s,\Delta T}$ reaches the maximum in Fig.4 which corresponds to the maximum total entropy angle difference between absorbing heat line and releasing heat line in Fig.3. The lower the $T_{c,in}/T_{h,in}$ under the condition of equal thermal capacity flow rates or heat exchange amount, the larger the total entropy angle difference between heat absorbing and releasing lines. So, the maximum value of $N_{s,\Delta T}$ increases with $T_{c,in}/T_{h,in}$ decreasing in Fig.4 which is consistent with the analysis of Eq. (7). Because *NTU* reaches 1 when $N_{s,\Delta T}$ reaches the maximum in Fig.4, it can be obtained that:

$$\dot{m}c_p\frac{T_{h,in}-T_{c,in}}{2}=\dot{m}c_p\Delta T_m \qquad (\dot{m}_c c_{p,c}=\dot{m}_h c_{p,h}, N_{s,\Delta T}=N_{s,\Delta T,max}) \tag{8}$$

Therefore, the average heat transfer temperature difference is half of the inlet temperature difference between two sides when $N_{s,\Delta T}$ reaches the maximum under equal thermal capacity flow rates.

To summarize, ε and $N_{s,\Delta T}$ don't show a consistent variation trend when *NTU* changes. However, the change of ε and $N_{s,\Delta T}$ can be reflected by the relative position of $T_{h,out}$ and $T_{c,out}$ in the line connecting $T_{h,in}$ and $T_{c,in}$ in *T-Q* diagram. Because $N_{s,\Delta T}$ increases with $T_{c,in}/T_{h,in}$ decreasing, a further conclusion can be obtained by using Fig.3 and Fig.4 is that $N_{s,\Delta T}$ increases with thermal capacity flow rate decreasing, heat exchange increasing, and inlet temperature average of both sides decreasing. But

$T_{c,in}/T_{h,in}$ doesn't change the variation trend of $N_{s,\Delta T}$. In most cases, the inlet temperatures of both streams are uncontrolled. Actually, the focus concerned by this study is the dimensionless form of $N_{s,\Delta T}$ relative to the peak value $N_{s,\Delta T,max}$. The increase of $N_{s,\Delta T}$ with *NTU* is evitable while *NTU* is less than 1. However, $N_{s,\Delta T}$ change is consistent with ε while *NTU* is larger than 1. Thus, for comprehensively considering the effect of heat exchanger effectiveness and heat transfer irreversibility, it can be given that:

$$\tau_2 = \begin{cases} \varepsilon & NTU < 1 \\ \frac{1}{2}\left(1 + \frac{N_{s,\Delta T,max} - N_{s,\Delta T}}{N_{s,\Delta T,max}}\right) & NTU \geq 1 \end{cases} \tag{9}$$

2.3. A new controlled variable

As discussed above, the terminal temperature difference changes caused by heat transfer irreversibility $N_{s,\Delta T}$ are equal at both ends. But the remanent irreversibility $N_{s,imb}$ makes the terminal temperature difference of one end deviate from the other.

Deriving from the *T*-*Q* diagram analysis in section 2.1, the Eq. (5), which reflects the effect of thermal capacity flow rate imbalance of both sides, can be transformed as:

$$\tau_1 = 1 - \left(\frac{(T_{h,out} - T_{c,in}) - (T_{h,in} - T_{c,out})}{T_{h,in} - T_{c,in}}\right)^2 \tag{10}$$

τ_1 reflects the imbalance extent of thermal capacity flow rates at both sides. When the thermal capacity flow rates of both sides are equal, τ_1 equals to 1 based on Eq. (6). As the thermal capacity flow rate difference between two sides increases, the imbalance extent of terminal temperature difference between two ends enlarges. As a result, τ_1 decreases. τ_1 approaches the minimum value, i.e. zero, in two situations. For the first situation, $T_{h,out}$ approaches $T_{c,in}$ and $T_{c,out}$ stays near $T_{c,in}$ due to the thermal capacity flow rate of cold stream being far larger than the hot side. For the second situation, $T_{c,out}$

approaches $T_{h,in}$ and $T_{h,out}$ stays near $T_{h,in}$ because of the thermal capacity flow rate of cold stream being far smaller than the hot side.

Based on the above *T-Q* diagram analysis in section 2.2, the Eq. (9), which reflects the effect of heat transfer irreversibility and heat exchanger effectiveness, can be transformed as:

$$\tau_2 = \frac{1}{2}\left(1 + \frac{T_{c,out} - T_{h,out}}{T_{h,in} - T_{c,in}}\right) \tag{11}$$

Here we consider the situation with equal thermal capacity flow rates. When *NTU* is 0, $T_{c,out}$=$T_{c,in}$ and $T_{h,out}$=$T_{h,in}$. According to Eq. (11), τ_2 equals 0. As *NTU* increases with heat exchange amount rising, $T_{c,out}$ moves towards $T_{h,in}$ and $T_{h,out}$ towards $T_{c,in}$ along the line connecting $T_{h,in}$ and $T_{c,in}$ in Fig.3 which leads to τ_2 increasing. Once $T_{c,out}$ meets $T_{h,out}$ in Fig.3, τ_2 reaches 0.5 which is the same with ε.

After $T_{c,out}$ meets $T_{h,out}$, $T_{c,out}$ continues to move towards $T_{h,in}$ and $T_{h,out}$ towards $T_{c,in}$ with *NTU* rising, indicating a larger τ_2. Because the overlap section of hot and cold stream temperature lines increases in Fig.3, the entropy generation reduces. At last, when $T_{h,out}$ reaches $T_{c,in}$ and $T_{c,out}$ reaches $T_{h,in}$, τ_2 reaches the maximum value, i.e. 1, which is the same with ε in Fig.4. Meanwhile, *NTU* approaches infinity and the entropy generation number decreases to be zero.

In summary, the change of τ_2 is consistent with the variation of ε in the case of equal thermal capacity flow rates. τ_2 has the consistent change trend with $N_{s,\Delta T}$ after *NTU* is larger than 1. Moreover, τ_2 also can indicate the influence of unequal thermal capacity flow rates. As discussed in section 2.1, the variation of thermal capacity flow rate difference will change $T_{h,out}$ and $T_{c,out}$ to different extent, which can be reflected by Eq. (11) as well.

A new controlled variable τ combining τ_1 with τ_2 is proposed:

$$\tau = \tau_2\tau_1 = \frac{1}{2}\left(1 + \frac{T_{c,out} - T_{h,out}}{T_{h,in} - T_{c,in}}\right)\left(1 - \left(\frac{(T_{h,out} - T_{c,in}) - (T_{h,in} - T_{c,out})}{T_{h,in} - T_{c,in}}\right)^2\right) \tag{12}$$

τ is named as the heat exchanger comprehensive effectiveness in this paper. In the case of equal thermal capacity flow rates, τ_1 equals to 1. τ_2 and τ increase from 0 to 1 with heat exchange amount rising. Because τ_2 is consistent with the variation of ε and $N_{s,\Delta T}$ after *NTU* is larger than 1, τ is as well.

In another situation where *NTU* approaches infinity, when the thermal capacity flow rates of both sides are equal, τ_1 and τ_2 both equal to 1. As the difference of thermal capacity flow rates is enlarged, τ_1 decreases from 1 to 0. Meanwhile, τ_2 decreases from 1 to 0.5 which is viewed as a compromise between the smaller side of thermal capacity flow rate approaching the maximum heat exchange and the larger side approaching the minimum heat exchange. As a comprehensive result, τ decreases from 1 to 0.

The advantages to introduce τ as the controlled variable are multifold. Firstly, τ only depends on the inlet and outlet temperatures. They are easy to be measured. Secondly, it can reflect simultaneously the influence of heat exchanger effectiveness ε, remanent irreversibility $N_{s,imb}$, and heat transfer irreversibility $N_{s,\Delta T}$ on the heat transfer efficiency.

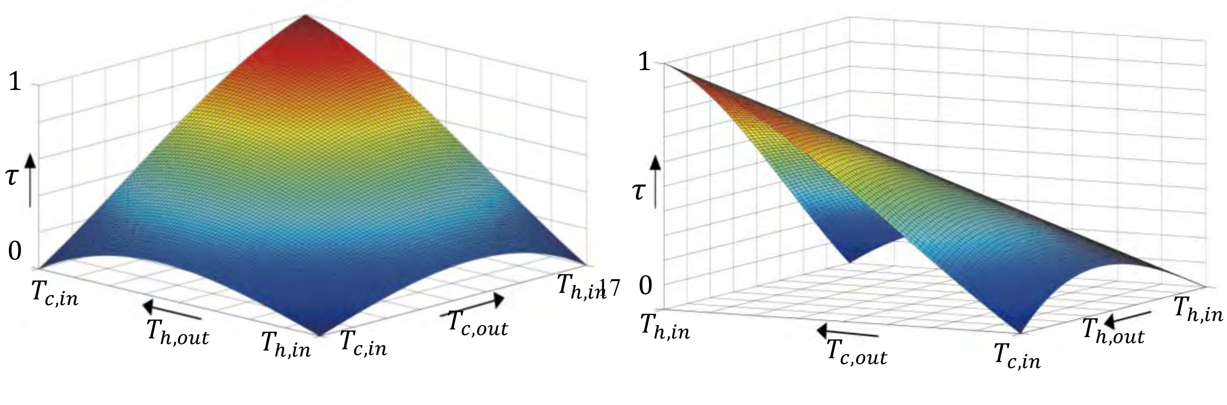

Fig.5 The change characteristics of τ with $T_{h,out}$ and $T_{c,out}$

Fig.5 shows the change characteristics of τ with $T_{h,out}$ and $T_{c,out}$. There are three points where τ is 0. At one point, $T_{h,out}$ holds at $T_{h,in}$ and $T_{c,out}$ holds at $T_{c,in}$. It means that *NTU* and heat exchange are 0. At the second point, $T_{h,out}$ maintains at $T_{h,in}$ and $T_{c,out}$ reaches $T_{h,in}$. It indicates the thermal capacity flow rate of the cold stream is far less than the hot. At the last point, $T_{c,out}$ holds at $T_{c,in}$ and $T_{h,out}$ reaches $T_{c,in}$. It means the thermal capacity flow rate of cold stream is far larger than the hot. Therefore, τ will be zero when *NTU* reaches 0 or the thermal capacity flow rates difference approaches the maximum.

When $T_{h,out}$ holds at $T_{h,in}$ and $T_{c,out}$ increases from $T_{c,in}$, τ firstly increases due to heat exchange amount increasing with *NTU* in Fig.5. On the other hand, the increase of $T_{c,out}$ enlarges the imbalance extent of terminal temperature difference between two ends which means the thermal capacity flow rate difference increases between two sides. As the effect of irreversible loss increasing, caused by a larger thermal capacity flow rate difference, finally exceeds that of heat exchange amount increment caused by *NTU* rising, τ reaches the peak value and then turns down to 0. It is the same in the case of $T_{c,out}$ holding at $T_{c,in}$ and $T_{h,out}$ decreasing from $T_{h,in}$ to $T_{c,in}$.

3. Results and discussion

The consistency of τ, ε and N_s is analyzed and validated. The change characteristics of controlled variable τ are compared with controlled variable $T_{h,out}$ by varying $T_{h,in}$ and $T_{c,in}$. Before the analysis, the thermal capacity flow rate ratio is defined as:

$$R = \frac{(\dot{m}c_p)_c}{(\dot{m}c_p)_h} \tag{13}$$

Based on Eq. (3) and Eq. (4), the entropy generation number N_s can be further expressed as:

$$N_s = \frac{(\dot{m}c_p)_c}{(\dot{m}c_p)_{min}} ln\,(\frac{T_{c,out}}{T_{c,in}}) + \frac{(\dot{m}c_p)_h}{(\dot{m}c_p)_{min}} ln\,(\frac{T_{h,out}}{T_{h,in}}) \quad (14)$$

3.1. Consistency analysis of τ, ε *and* N_s

In the section, two typical situations are discussed. In the first one, thermal capacity flow rate ratio varies under the scenario of *NTU* approaching infinity. In the second one, *NTU* changes in the case with equal thermal capacity flow rates. The inlet temperatures of hot and cold streams, for example, are maintained at 75°C and 15°C respectively. The response of τ, ε and N_s are compared.

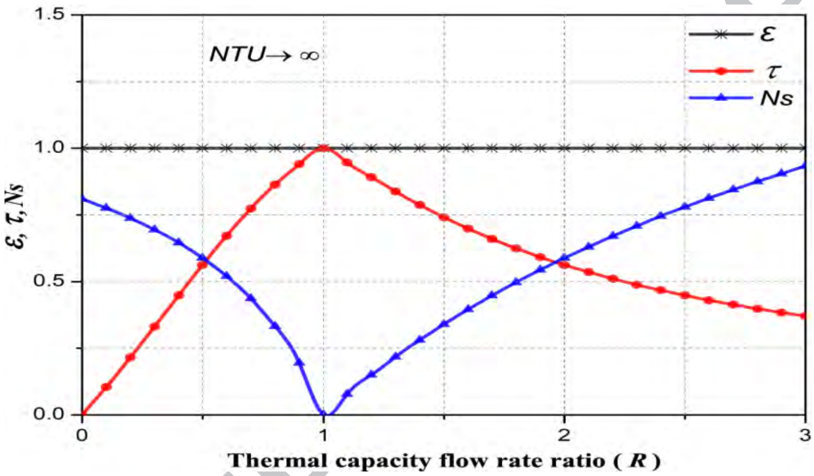

Fig.6 The variation of ε, τ *and* N_s with thermal capacity flow rate ratio (*NTU*->∞)

Fig.6 shows the variation of ε, τ and N_s with thermal capacity flow rate ratio when *NTU* approaching infinity. Because of *NTU* approaching infinity, the outlet temperature of the side with a smaller thermal capacity flow rate reaches the inlet temperature of the other side. As a result, ε is always one. Entropy generation number N_s firstly decreases due to $N_{s,imb}$ reducing with thermal capacity flow rate ratio R rising from 0 to 1. At the same time, τ increases. When *R* equals 1, N_s reaches the minimum and turns to increase due to $N_{s,imb}$ increasing. τ decreases after reaching the maximum where *R*=1. Clearly τ can reflect the change of N_s.

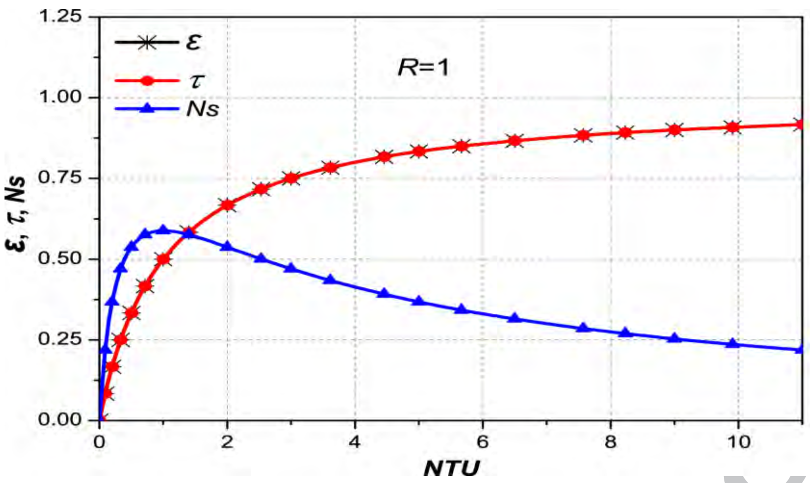

Fig.7 The variation of ε, τ *and* N_s with *NTU* (R=1)

The changes of ε, τ and N_s with *NTU* if *R*=1 are shown in Fig.7. Here ε is restricted by thermal resistance which also influences $N_{s,\Delta T}$. As *NTU* increases, heat transfer is enhanced which leads to ε rising. N_s increases firstly due to heat exchange amount rising and then decreases due to $N_{s,\Delta T}$ decreasing. The line of τ overlaps with that of ε. Therefore, τ considers the effects of both ε and N_s. τ also shows a good accordance with ε and N_s.

3.2. Comparative analysis of controlled variable τ *and* $T_{h,out}$ *with* $T_{h,in}$

The cold stream inlet temperature $T_{c,in}$, for instance, is maintained at 15°C and hot stream inlet temperature $T_{h,in}$ increases from 60°C to 90°C. The responses of $T_{h,out}$ and τ as controlled variables are compared. Two extreme cases are introduced. One is keeping thermal capacity flow rate ratio *R* unchanged. The other is keeping *NTU* constant. Actually, in the real processes, *NTU* normally increases with thermal capacity flow rate. Therefore, the values of ε, τ, N_s *and* $T_{h,out}$ in real processes range between these two extreme cases.

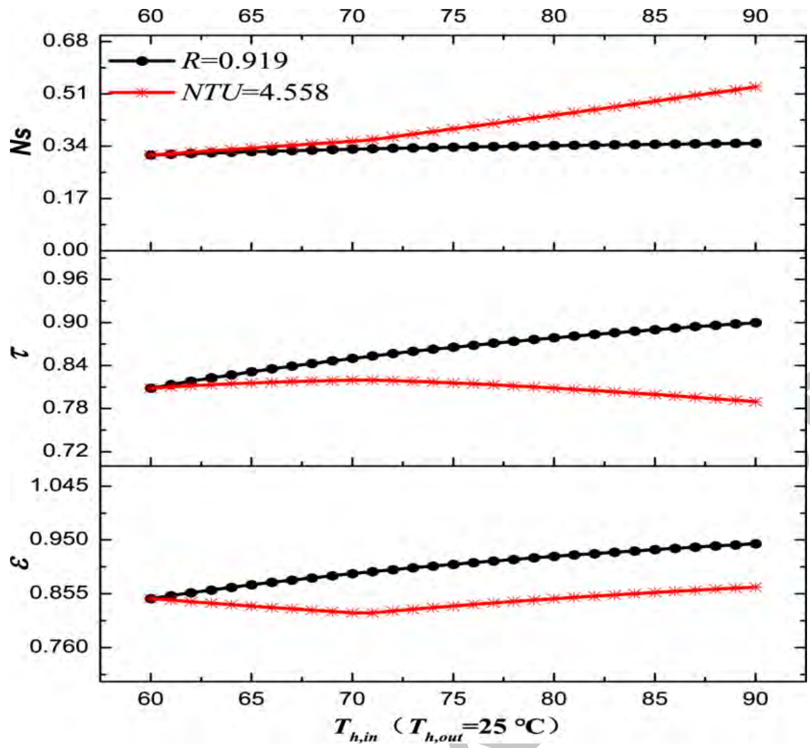

Fig.8 The variation of ε, τ *and* N_s with $T_{h,in}$ when selecting $T_{h,out}$ as controlled variable

Fig.8 shows that N_s and ε have obvious change with $T_{h,in}$ when controlling $T_{h,out}$ at 25℃. In the case of *R*=0.919, N_s increases slightly. τ follows the increase of ε. In the case of *NTU*=4.558, ε decreases a little at the beginning. Meanwhile, N_s increases very slowly. Combining the effect of ε and N_s, τ changes very little. Then as N_s rapidly increases, the effect of N_s on heat exchange efficiency exceeds ε which results in the drop of τ.

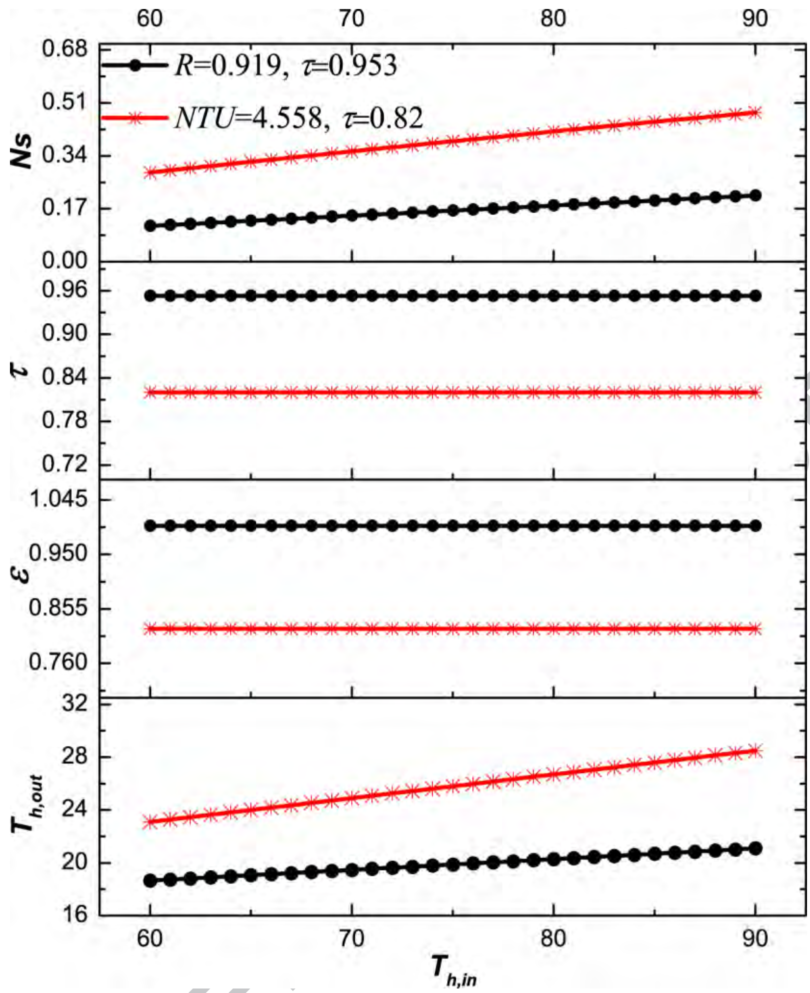

Fig.9 The variation of $T_{h,out}$, ε *and* N_s with $T_{h,in}$ when selecting τ as controlled variable

Table 1 Comparison of parameters variation range of different controlled variables in the case where $T_{h,in}$ changes

Control Variable	Condition	$T_{h,out}$ (℃)	τ	ε	N_s
$T_{h,out}$	R=0.919	25	0.808~0.9	0.847~0.943	0.311~0.349
$T_{h,out}$	*NTU*=4.558	25	0.82~0.79	0.821~0.867	0.311~0.533
τ	R=0.919	18.656~21.093	0.953	1	0.115~0.213
τ	*NTU*=4.558	23.096~28.494	0.82	0.82	0.287~0.479

Fig.9 shows the parameters variation with $T_{h,in}$ when adopting τ as controlled variable. The curves of two extreme cases shown in Fig.8 and Fig.9 indicate the lower limit and upper limit of parameters in real processes. Table. 1 compares the variation range of parameters under two extreme cases with different controlled variables. Compared to $T_{h,out}$, the upper limit of ε is raised when selecting τ as controlled variable, which means stronger heat transfer can be obtained. Compared to controlled variable $T_{h,out}$, the lower and upper limit of N_s both decrease obviously when adopting τ as controlled variable, pushing the irreversible loss down to a lower value. To summarize, controlled variable τ can achieve higher ε and lower N_s.

3.3. Comparative analysis of controlled variable τ *and* $T_{h,out}$ *with* $T_{c,in}$

Here the hot stream inlet temperature $T_{\mathrm{h},in}$ is kept at 75℃ as an example. The cold stream inlet temperature $T_{c,in}$ increases from 5℃ to 20℃. Controlled variables $T_{h,out}$ and τ, like section 3.2, are compared under two extreme cases. One is keeping thermal capacity flow rate ratio unchanged. The other is keeping *NTU* constant. It is the same that the parameter values of real processes range between the two extreme cases.

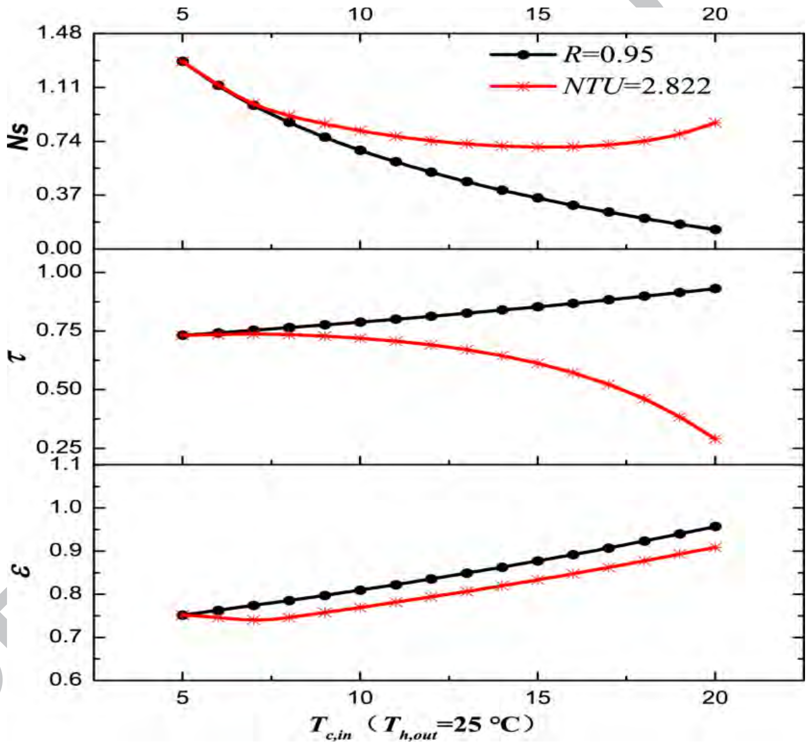

Fig.10 The parameters variation with $T_{c,in}$ when selecting $T_{h,out}$ as controlled variable

As shown in Fig.10, controlling $T_{h,out}$ at 25℃, N_s and ε change remarkably with $T_{c,in}$. In the case of *R*=0.95, the decrease of N_s and the increase of ε result in the increase of τ. In the case of *NTU*=2.822, the rise delay of ε and the decrease of N_s just cause a tiny change of τ at the beginning. After N_s goes down to the low limit and then turns to increase, the effect of N_s increasing gradually exceeds ε increasing. As a result, τ decreases.

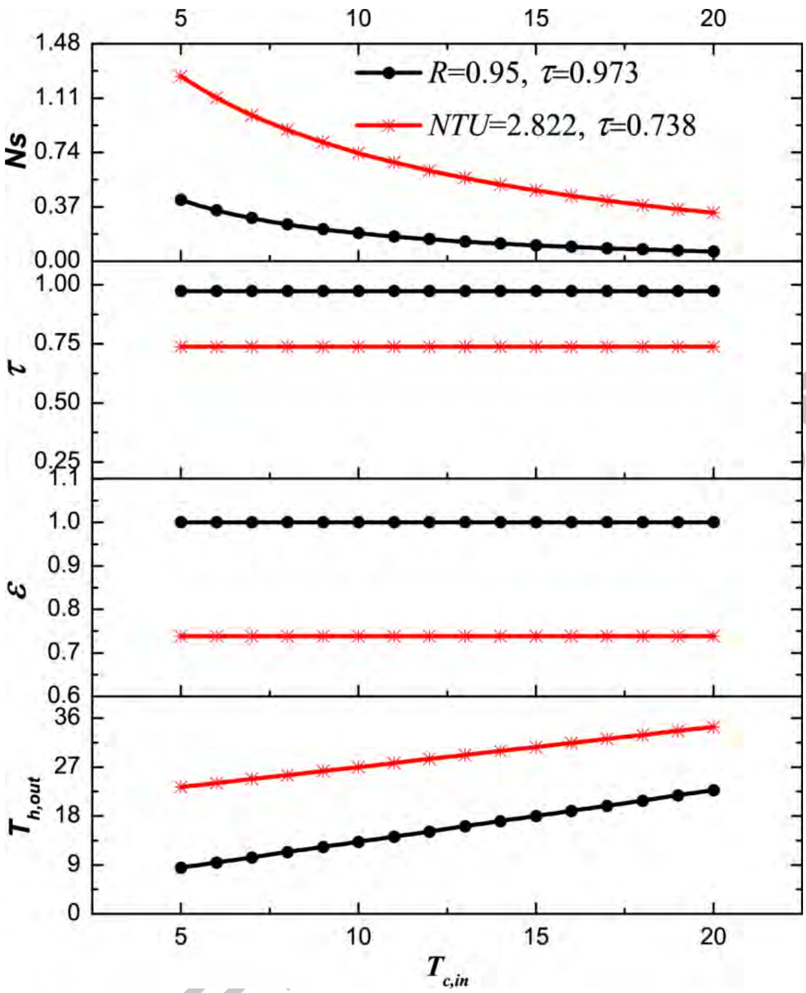

Fig.11 The parameters variation with $T_{c,in}$ when selecting τ as controlled variable

Table 2 Comparison of parameters variation range of different controlled variables in the case where $T_{C,in}$ changes

Control Variable	Condition	$T_{h,out}$ (℃)	τ	ε	N_s
$T_{h,out}$	R=0.95	25	0.732~0.931	0.752~0.957	1.288~0.1332
$T_{h,out}$	*NTU*=2.822	25	0.738~0.29	0.74~0.909	1.288~0.7
τ	R=0.95	8.5~ 22.75	0.973	1	0.416~ 0.066
τ	*NTU*=2.822	23.317~ 34.392	0.738	0.738	1.26~ 0.329

Fig. 11 shows the change of parameters with $T_{c,in}$ when adopting τ as controlled variable. The curves in Fig.10 and Fig.11 form the lower and upper limit of parameters in real processes. Table. 2 compares the variation range of parameters under different controlled variables. The upper limit of ε in the case using controlled variable τ is higher than that of $T_{h,out}$, thus stronger heat transfer can be achieved. N_s decreases monotonously when *NTU*=2.822 in Fig.11. It is different from the result in Fig.10. Compared to controlled variable $T_{h,out}$, the lower and upper limit of N_s in the case using controlled variable τ both significantly reduced, which limits the irreversible loss to a lower value. In sum, controlled variable τ can achieve higher ε and lower N_s than controlled variable $T_{h,out}$.

4. Conclusions

Based on maximizing the heat exchange amount and minimizing the irreversible loss, a new controlled variable of counter flow heat exchanger, i.e. heat exchanger comprehensive effectiveness τ, is constructed by using *T*-*Q* diagram inducing entropy angle and thermal capacity angle. The *T*-*Q* diagram can more clearly reflect the relation between heat exchanger effectiveness ε, heat transfer irreversibility $N_{s,\Delta T}$, and remanent irreversibility $N_{s,imb}$.

- Selecting the outlet temperature of one side stream as controlled variable has its limitations. It is incapable of perceiving all changes of thermal capacity flow rates.
- The heat exchanger effectiveness ε doesn't show a completely consistent change trend with heat transfer irreversibility $N_{s,\Delta T}$, and couldn't reflect the influence of remanent irreversibility $N_{s,imb}$.
- The terminal temperature differences imposed by heat transfer irreversibility $N_{s,\Delta T}$ at both ends are the same. The remanent irreversibility $N_{s,imb}$ results in that the terminal temperature difference of one end deviates from the other.
- The new controlled variable τ is easy to be measured and can reflect the effect of heat exchanger effectiveness, remanent irreversibility, and heat transfer irreversibility simultaneously.

Acknowledgements

The authors would like to acknowledge the financial support by the Fundamental Research Funds for the Central Universities, ENN-Tongji Institute for Advanced Clean Energy, and National Fundamental Research Program 973 project (2014CB249201) "Research on the stability of complex energy system

integrated natural gas and renewable energy".

References

[1] Arbaoui M A, Vernières-Hassimi L, Seguin D, Abdelghani-Idrissi M A. Counter-current tubular heat exchanger: Modeling and adaptive predictive functional control. Applied Thermal Engineering 2007; 27: 2332–2338.

[2] Abu-Hamdeh N H. Control of a liquid-liquid heat exchanger. Heat and Mass Transfer 2002; 38: 687-693.

[3] Heo S, Jogwar S S, Daoutidis P. Dynamics and control of high duty counter-current heat exchangers, 19th Mediterranean Conference on Control and Automation, 2011, 1034-1039.

[4] Maidi A, Diaf M, Corriou J. Boundary geometric control of a counter-current heat exchanger. Journal of Process Control 2009; 19: 297-313.

[5] Burns J A, Zietsman L, Control of a thermal fluid heat exchanger with actuator dynamics, 55th IEEE Conference on Decision and Control, 2016, 3131-3136.

[6] Burns J A, Herdman T L, Zietsman L. Approximating parabolic boundary control problems with delayed actuator dynamics, American Control Conference, 2013, 2080-2085.

[7] Burns J A, Kramer B. Full flux models for optimization and control of heat exchangers, American Control Conference, 2015, 577-582.

[8] Burns J A, Cliff E M. Numerical methods for optimal control of heat exchangers, American Control Conference, 2014, 1649-1654.

[9] Ansari M R, Mortazavi V. Simulation of dynamical response of a countercurrent heat exchanger to inlet temperature or mass flow rate change. Applied Thermal Engineering 2006; 26: 2401-2408.

[10] Feru E, Willems F, Rojer C, et al. Heat exchanger modeling and identification for control of waste heat recovery systems in diesel engines, American Control Conference, 2013, 2860-2865.

[11] Lakshmanan C C, Potter O E. Dynamic simulation of a countercurrent heat exchanger modelling-start-up and frequency response. International Communications in Heat and Mass Transfer 1994; 21: 421-434.

[12] Abdelghani-Idrissi M A, Bagui F, Estel L. Analytical and experimental response time to flow rate step along a counter flow double pipe heat exchanger. Heat and Mass Transfer 2001; 44: 3721-3730.

[13] Laskowski R. The black box model of a double-tube counter-flow heat exchanger. Heat Mass Transfer 2015; 51:1111–1119.

[14] Naphon P. Second law analysis on the heat transfer of the horizontal concentric tube heat exchanger. International Communications in Heat and Mass Transfer 2006; 33: 1029-1041.

[15] Manjunath K, Kaushik S C. Second law thermodynamic study of heat exchangers: A review. Renewable and sustainable energy reviews 2014; 40: 348-374.

[16] Lerou P P P M, Veenstra T T, Burger J F, Brake ter H J M, Rogalla H. Optimization of counter flow heat exchanger geometry through minimization of entropy generation. Cryogenics 2005; 45: 659–669.

[17] Ordonez J C, Bejan A. Entropy generation minimization in parallel-plates counter flow heat exchangers. Int J Energy Res 2000;24:843–864.

[18] Mohamed H A. Entropy generation in counter flow gas to gas heat exchangers. J Heat Transf 2006; 128:87–92.

[19] Xu Z M, Liu Z D, Zhang Y L. Irreversibility and available energy loss in a heat exchanger. Int J Heat Mass Transf 2015; 88: 552–557.

[20] San J Y. Second-law performance of heat exchangers for waste heat recovery. Energy 2010; 35: 1936-1945.

[21] Gupta P K , Kush P K, Tiwari Ashesh. Second law analysis of counter flow cryogenic heat exchangers in presence of ambient heat-in-leak and longitudinal conduction through wall. Int J Heat Mass Transf 2007; 50: 4754–66.

[22] Bejan A. The concept of irreversibility in heat exchanger design: counter flow heat exchangers for gas-to-gas applications. J Heat Transf 1977; 99:374–80.

[23] Bahadori A. Simple method for estimation of effectiveness in one tube pass and one shell pass counter-flow heat exchangers. Applied Energy 2011; 88: 4191-4196.

[24] Bejan A. Advanced Engineering Thermodynamics. 1st ed.. New York: Wiley; 1988.

Table 1 Comparison of parameters variation range of different controlled variables in the case where $T_{h,in}$ changes

Control Variable	Condition	$T_{h,out}$ (℃)	τ	ε	N_s
$T_{h,out}$	R=0.919	25	0.808~0.9	0.847~0.943	0.311~0.349
$T_{h,out}$	*NTU*=4.558	25	0.82~0.79	0.821~0.867	0.311~0.533
τ	R=0.919	18.656~21.093	0.953	1	0.115~0.213
τ	*NTU*=4.558	23.096~28.494	0.82	0.82	0.287~0.479

Table 2 Comparison of parameters variation range of different controlled variables in the case where $T_{C,in}$ changes

Control Variable	Condition	$T_{h,out}$ (℃)	τ	ε	N_s
$T_{h,out}$	R=0.95	25	0.732~0.931	0.752~0.957	1.288~0.1332
$T_{h,out}$	*NTU*=2.822	25	0.738~0.29	0.74~0.909	1.288~0.7
τ	R=0.95	8.5~ 22.75	0.973	1	0.416~ 0.066
τ	*NTU*=2.822	23.317~ 34.392	0.738	0.738	1.26~ 0.329

Highlights

- Optimal controlled variable of counter flow heat exchanger is constructed.
- T-Q diagram analysis inducing entropy angle and thermal capacity angle is proposed.
- Different effect of remanent irreversibility and heat transfer irreversibility on terminal temperature difference is identified.
- Difference between heat exchanger effectiveness, heat transfer irreversibility and remanent irreversibility is obtained.